

Disclaimer: This is not the final version of the article. Changes may occur when the manuscript is published in its final format.

1 Preparation and Characterization of Biocompatible Hydrogels based on a

2 Chitosan-Polyacrylamide Copolymer

3

4 **Elena Rosova** elenarosova@hotmail.com Institute of Macromolecular Compounds - Branch of
5 Petersburg Nuclear Physics Institute named by B.P. Konstantinov of National Research Centre
6 «Kurchatov Institute», St. Petersburg, Bolshoy pr., 31, 199004, Russia 0000-0002-8608-3024

7 **Zoolsho Zoolshoev** zoolfar@mail.ru Institute of Macromolecular Compounds - Branch of
8 Petersburg Nuclear Physics Institute named by B.P. Konstantinov of National Research Centre
9 «Kurchatov Institute», St. Petersburg, Bolshoy pr., 31, 199004, Russia 0000-0002-4533-5125

10 **Ekaterina Vyrezkova** kate_vy@mail.ru St. Petersburg State Technological Institute (Technical
11 University), St. Petersburg, Moskovski pr., 26, 190013, Russia

12 **Elena Vlasova** evl021960@gmail.com Institute of Macromolecular Compounds - Branch of
13 Petersburg Nuclear Physics Institute named by B.P. Konstantinov of National Research Centre
14 «Kurchatov Institute», St. Petersburg, Bolshoy pr., 31, 199004, Russia 0000-0002-4644-0445

15 **Natalia Smirnova** nvsmirnoff@yandex.ru Institute of Macromolecular Compounds - Branch of
16 Petersburg Nuclear Physics Institute named by B.P. Konstantinov of National Research Centre
17 «Kurchatov Institute», St. Petersburg, Bolshoy pr., 31, 199004, Russia 0000-0001-5524-2785

18 **Konstantin Kolbe** kkolbe@yandex.ru Institute of Macromolecular Compounds - Branch of
19 Petersburg Nuclear Physics Institute named by B.P. Konstantinov of National Research Centre
20 «Kurchatov Institute», St. Petersburg, Bolshoy pr., 31, 199004, Russia 0000-0002-2304-1759

21 **Natalia Saprykina** elmic@hq.macro.ru Institute of Macromolecular Compounds - Branch of
22 Petersburg Nuclear Physics Institute named by B.P. Konstantinov of National Research Centre
23 «Kurchatov Institute», St. Petersburg, Bolshoy pr., 31, 199004, Russia
24 0000-0002-9240-1690

25 **Ivan Kuryndin** isk76@mail.ru Institute of Macromolecular Compounds - Branch of Petersburg
26 Nuclear Physics Institute named by B.P. Konstantinov of National Research Centre «Kurchatov
27 Institute», St. Petersburg, Bolshoy pr., 31, 199004, Russia 0000-0003-0613-9460

28

29

30 *Corresponding author, e-mail: isk76@mail.ru

31

32

33

34

35

36

37

38 Abstract

Disclaimer: This is not the final version of the article. Changes may occur when the manuscript is published in its final format.

39 Hydrogels comprised of natural and synthetic polymers are widely used in the biomedical
40 field due to their distinguishing properties, such as softness, flexibility, swelling, and
41 biocompatibility. In this study, we obtained and characterized hydrogel materials based on
42 chitosan/acrylamide copolymer as potential matrices for biomedical applications. FTIR studies
43 confirmed the formation of chitosan/polyacrylamide graft copolymer. Kinetics of gel formation
44 was investigated with the rheological tests and the change of reaction mixture viscosity in the
45 shear mode was measured. Scanning electron microscopy revealed a porous surface with micron-
46 and submicron-sized gels. The kinetics of swelling/drying processes in the obtained hydrogels
47 were studied at varying pH values. A significant decrease in the equilibrium swelling degree in
48 an alkaline medium was observed, dropping from 50 g/g in the first cycle to 36 g/g in the second
49 cycle. Mechanical characteristics of the chitosan/polyacrylamide hydrogel-shaped samples were
50 tested both in compression and tension modes. It was found that for the samples swollen at pH
51 6.8, the tensile and compression strengths were 37 kPa and 19 kPa, respectively. The biological
52 activity of the obtained hydrogels was evaluated by the MTT test. The Kinetics of drug release
53 from hydrogels in phosphate buffer was studied using lidocaine hydrochloride as a model
54 compound.

55

56 **Keywords:** hydrogels; polyacrylamide; chitosan; swelling; biocompatibility

57

58 **1. Introduction**

59

60 Currently, a large number of research works are devoted to the development and preparation of
61 new biomaterials with attractive applications in different fields [1,2,3].

62 Special attention was paid to swelling hydrogels based on natural and synthetic polymers,
63 which can be used independently as matrices for the formation of composites with various
64 functional and physico-mechanical properties [4,5,6]. Hydrogel-based materials of specific

Disclaimer: This is not the final version of the article. Changes may occur when the manuscript is published in its final format.

65 geometric shapes and purposes are used in cosmetology, biotechnology, tissue engineering,
66 medicine, and pharmaceuticals [7,8,9]. The presence of a natural component in a hydrogel
67 significantly increases the biocompatibility of these hybrid systems and the possibility of their
68 biomedical application [10,11,12]. The most common and inexpensive natural polymers are
69 polysaccharides, such as cellulose, chitosan, lignin, collagen, and gelatin [13,14]. Along with the
70 absence of toxicity, they are characterized by biocompatibility, coagulation ability, and the
71 ability to adsorb biopharmaceuticals [15,16]. Among the polymers listed above, chitosan fully
72 meets the requirements for biomaterials used in medicine, cosmetology, and tissue engineering
73 [17,18,19]. It will be recalled that the preparation of chitosan-based hydrogels (the formation of a
74 crosslinked structure) requires the use of toxic synthetic or expensive natural crosslinkers
75 [20,21,22]. A possible solution to this problem is to obtain hybrid systems based on synthetic
76 polymers, which enhance mechanical strength by cross-linking macromolecules through
77 transverse covalent bonds and forming a three-dimensional network [23,24]. This approach
78 allows for expanding possible applications of chitosan and other natural polymers.

79 The choice of a synthetic polymer for the preparation of a hybrid material is limited by
80 the fact that synthesis or processing of these materials is usually carried out in high-temperature
81 melts or solutions in organic solvents, which precludes the possibility of combining them with
82 natural polymers [25]. In this connection, the class of water-soluble synthetic polymers (or
83 polymers synthesized in an aqueous environment) attracts much interest. Among water-soluble
84 monomers, acrylamide deserves special attention because the polymers based on it are
85 biocompatible, hydrophilic, and have good film-forming properties [26,27,28].

86 N, N'-Methylene-bis-acrylamide is widely used as a crosslinking agent for synthesizing
87 spatially crosslinked structures of acrylamide. Crosslinked polyacrylamide, due to the presence
88 of hydrophilic groups and a three-dimensional framework, is a hydrogel capable of absorbing
89 large amounts of water, aqueous solutions, and biological fluids [29,30].

Disclaimer: This is not the final version of the article. Changes may occur when the manuscript is published in its final format.

90 Acrylamide is known to form copolymers with hydrophilic and hydrophobic monomers.
91 Graft copolymerization of acrylamide can be used both to modify existing polymers and to
92 obtain new cross-linked hybrid structures [31,32].

93 Hydrogels based on natural, semi-synthetic, and synthetic polymers are considered
94 innovative materials for biomedical applications. Hydrophilicity, swelling, biocompatibility,
95 mechanical stability, and desired flexibility allow hydrogels to be considered promising drug
96 delivery systems [33]. Compared to other materials such as nanocapsules, micelles, and
97 liposomes, hydrogels exhibit higher drug-loading capacity and provide controlled drug release
98 [34,35].

99 Hydrogels based on polyacrylamide/chitosan copolymer have been studied sufficiently. At the
100 same time, copolymer hydrogel materials with different functional properties are still of interest
101 to specialists in medical and biotechnological fields including the design of contact lenses,
102 hygiene products, tissue engineering scaffolds, drug delivery systems, and wound dressings [36].
103 The advantage of these materials lies in their ability to be fabricated into various geometric
104 shapes and sizes during production, depending on the specific application. Additionally, they
105 offer softness, flexibility, and a high degree of transparency [37,38]. The above-mentioned
106 properties make these materials promising for use in ophthalmology [39], and the resulting films
107 with a different thickness and surface area could potentially be used as skin care treatment
108 materials. Mechanical properties are important characteristics of hydrogel materials in their
109 further use for biomedical and cosmetic applications. [40]. Improving the mechanical
110 characteristics of hydrogels by modifying the input polymers or introducing fillers often leads to
111 a loss of transparency of the gel or the acquisition of color, whereas for several applications these
112 properties are crucial [41, 42].

113 The aim of this work was to obtain hydrogel materials based on polyacrylamide/chitosan
114 copolymer in the form of cylinders and thin films with appropriate mechanical properties in the
115 swollen state, lack of cytotoxicity and bioactivity, as well as the ability to drug release.

Disclaimer: This is not the final version of the article. Changes may occur when the manuscript is published in its final format.

116

117 **2. Materials and Methods**

118

119 **2.1. Materials**

120 The copolymers based on polyacrylamide (PAA) and chitosan were prepared by graft
121 copolymerization of acrylamide (AA) (SIGMA-ALDRICH, 98%) in solutions of chitosan (LLC
122 «Bioprocess», $M_w = 80 \cdot 10^3$ g/mol, DD 90%) in acetic acid (99.8%, Vecton, St-Petersburg,
123 Russia). The polymerization was initiated by ammonium peroxydisulfate (APS) (SIGMA-
124 ALDRICH, 98%) and N, N, N', N'-tetramethylethylenediamine (TEMED) (SIGMA-ALDRICH,
125 99%) [31].

126

127 **2.2. Synthesis of polyacrylamide/chitosan hydrogels**

128 Hydrogels were synthesized from acrylamide and chitosan by the addition of a crosslinking
129 agent (N, N'-methylene-bis-acrylamide, MBAA, SIGMA-ALDRICH, 98%) at the grafting stage.

130 To synthesize hydrogels, 30% aqueous solution of the monomer (AA) was mixed with
131 1% aqueous solution of the crosslinking agent (MBAA) in the 10:1 ratio (v/v). Then, 1%
132 solution of chitosan in 0.1 M acetic acid (8:2 v/v), TEMED, and APS were added to the reaction
133 mixture [36].

134

135 **2.3. Rheological tests**

136 The kinetics of gel formation was investigated using the rheological method by measuring the
137 change in viscosity of the reaction mixture at 25°C under the shear mode. The measurements
138 were carried out on a "Reotest-2" rotational viscometer (VEB MLW, Germany) with a
139 thermostated cylinder-cylinder working unit (the ratio of cylinder radii was equal to 1.24) at a
140 shear rate of 5.4 s⁻¹.

141

Disclaimer: This is not the final version of the article. Changes may occur when the manuscript is published in its final format.

142 2.4. Obtaining the samples

143 To obtain hydrogel samples, the prepared reaction mixture was poured into an appropriate mold,
144 namely, the test tubes, and into the cell with plane-parallel sides with a variable gap. The
145 gelation process was carried out in air at room temperature for 24 hours. Then the gel was taken
146 out of the mold and washed in distilled water to remove the residues of acrylamide and the
147 crosslinking agent. Therefore, the samples in the form of cylinders and films were obtained. For
148 further studies, the gels were dried in air to constant weight and then placed in a vacuum drying
149 oven until the moisture was completely removed.

150

151 2.5. Morphology and transparency tests

152 The morphology of lyophilized samples was investigated using a SUPRA-55VP scanning
153 electron microscope (ZEISS, Germany). Gel transparency was determined on a UV-vis
154 spectroscopy on an SF-2000 (OKB Spectr, Russia) spectrometer. The measurements were
155 carried out at different sections of the sample at least 5 times, and the variation of values did not
156 exceed 2%.

157

158 2.6. FTIR spectra

159 FTIR spectra of the gel samples were recorded on a Bruker Vertex70 spectrometer using a Pike
160 attenuated total reflectance (ATR) microattachment with a ZnSe working element. During
161 registration of the FTIR spectra, a correction was made that took into account the dependence of
162 penetration depth on wavelength.

163

164 2.7. Study of swelling/drying processes

165 Kinetics of swelling/drying processes in the hydrogels were studied in the media with different
166 pH values: 0.1 M HCl (pH 2.1), distilled water (pH 6.8), and 0.1 M NaOH (pH 12.8). The
167 samples dried in a vacuum to constant weight were placed in the solutions with a given pH at a

Disclaimer: This is not the final version of the article. Changes may occur when the manuscript is published in its final format.

168 gel/solution mass ratio of 1/1500 to ensure pH constancy during the swelling process. The
169 weight of the swelling samples was measured at fixed intervals. The swelling degree was
170 calculated according to the Eq. (1) [43]:

$$171 \quad Q = \frac{m - m_0}{m_0} \quad (1)$$

172 where m is the mass of the swollen sample (g) and m_0 is the mass of the initial dry sample (g).

173 The swelling process was considered to be completed when the gels reached the
174 equilibrium swelling degree (Q_e), which was characterized by the unchanged weight of a
175 hydrogel during further exposure to the liquid.

176 Gel drying (liquid desorption) was carried out in air at room temperature until a constant
177 weight was reached; the change in sample mass over time (Δm) was controlled. The mass of the
178 samples was determined gravimetrically with an Analytical balance VL-210 (Gosmetr, Russia).
179 Repeated swelling/drying cycles were performed to determine the reversibility of the processes.
180 Each swelling test was performed on at least 3 samples. The spread of swelling/drying degree
181 values was no more than 10 %.

182

183 2.8. Mechanical tests

184 The deformation behavior of hydrogels after their equilibrium swelling was investigated on a
185 2166 R-5 tensile testing machine (Tochpribor, Ivanovo, Russia). Cylindrical samples and film
186 samples were used for the tests in the uniaxial compression mode at a compression rate of 5
187 mm/min and in the uniaxial extension mode at a stretching rate of 40 mm/min, respectively. The
188 obtained stress-strain curves were used to determine the values of breaking strength, deformation
189 at break, and elastic modulus [44]. For each sample, the test was performed at least 5 times. The
190 spread of values of mechanical characteristics did not exceed 10% of their values. The Young's
191 modulus (E) corresponded to the elastic modulus under stretching:

$$192 \quad E = \frac{\sigma}{\varepsilon} \quad (2)$$

Disclaimer: This is not the final version of the article. Changes may occur when the manuscript is published in its final format.

193 where σ is the tensile stress, and ε is the axial strain.

194 The elastic modulus (G) under compression was calculated according to the following
195 formula:

$$196 \quad G = \frac{\sigma}{\lambda - \lambda^{-2}} \quad (3)$$

197 where σ is the stress, λ is the deformation at compression determined as the ratio of the current
198 sample height to the initial sample height.

199

200 2.9. Biocompatibility studies

201 The biological activity of the obtained hydrogels was evaluated using colorimetric analysis of
202 cell proliferation and cytotoxicity with 3-[4,5-dimethylthiazol-2-yl]-2,5-diphenyltetrazolium
203 bromide (MTT test). The adhesion efficiency, viability, proliferation, and morphology of human
204 dermal fibroblasts during cultivation on the chitosan/PAA hydrogel matrices were assessed. The
205 optical density of the solution was recorded using a SPECTROstar spectrophotometer (USA).
206 The absorbance of formazan was determined at 570 nm, and the cut-off wavelength was equal to
207 690 nm.

208

209 2.10. Drug release

210 Lidocaine hydrochloride (HL) solution was used as a model drug compound to study the release
211 process. For the incorporation of HL into hydrogels, the pre-dried samples were swollen in a
212 10% aqueous solution of HL to an equilibrium state. The gels were then extracted from the
213 solution, followed by the residual solution removed from the gel surface. Then the swollen
214 hydrogels were used in drug release experiments from hydrogels in a physiological solution (pH
215 7.4). The concentration of HL was determined by UV-vis spectroscopy at 37 °C and calculated
216 from the calibration dependences of the optical density on the concentration of HL at $\lambda = 264$
217 nm.

Disclaimer: This is not the final version of the article. Changes may occur when the manuscript is published in its final format.

218

219 **3. Results and discussion**

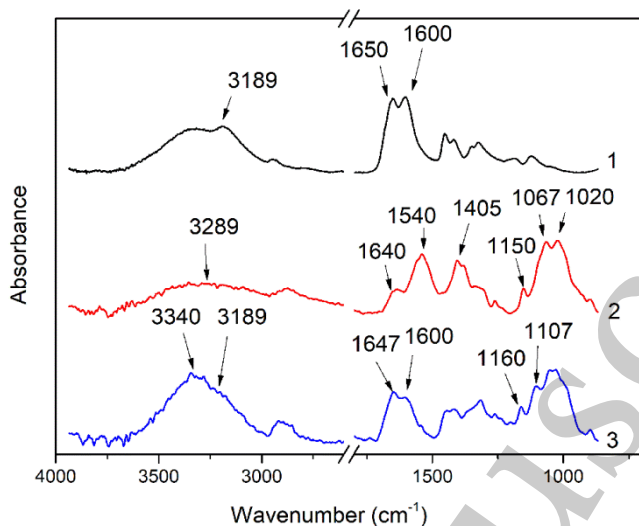
220

221 **3.1. Investigation of the gel formation process**

222 It has been previously shown that acrylic acid (AA) grafts onto chitosan through its amino and
223 hydroxyl groups. In this work, the formation of graft copolymers was confirmed by FTIR studies
224 [35, 36].

225 The FTIR spectra of PAA, chitosan, and chitosan/PAA copolymer are shown in Figure 1.
226 In the PAA spectrum (1), the bands at 3189 cm^{-1} (valence vibrations of NH_2 group in the primary
227 amide), 1650 cm^{-1} (C=O of the amide group), and 1600 cm^{-1} (deformation vibrations of NH_2
228 group in the primary amide) are observed. In the FTIR spectrum of chitosan (2) in the salt form,
229 the following characteristic bands can be detected: the wide band at $3500\text{--}3100\text{ cm}^{-1}$ (primary
230 and secondary OH groups, protonated NH_3^+ groups, NH of the secondary amide), and the peak at
231 1647 cm^{-1} (CO group of Amide I). The complex band with a maximum at 1540 cm^{-1} is a
232 superposition of three absorption bands: $1550\text{--}1560\text{ cm}^{-1}$ (Amide II), $1560\text{--}1530\text{ cm}^{-1}$
233 (protonated NH_3^+ groups), and $1590\text{--}1550\text{ cm}^{-1}$ (COO^- groups of acetate counterions). The
234 presence of acetate counterions is also confirmed by the appearance of the band at 1405 cm^{-1} .
235 The peak at 1150 cm^{-1} is assigned to the valence vibrations of the bridging oxygen; the bands in
236 the $1070\text{--}1020\text{ cm}^{-1}$ regions are attributed to C-O vibrations [45,46].

Disclaimer: This is not the final version of the article. Changes may occur when the manuscript is published in its final format.

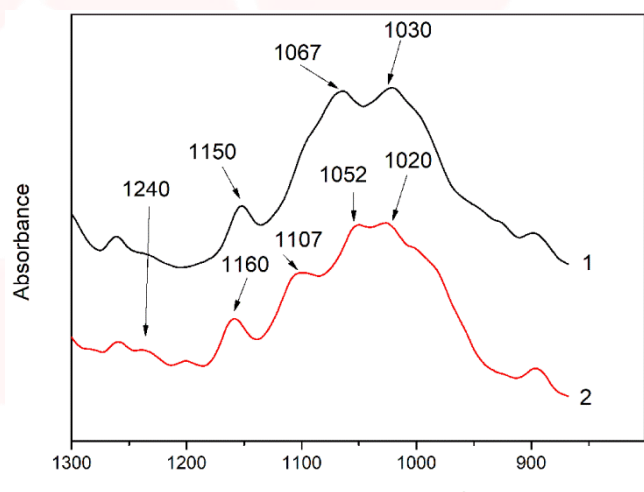


237

238 **Fig. 1.** FTIR spectra of PAA (1), chitosan (2), and the chitosan/PAA copolymer (3).

239

240 The FTIR spectrum of the chitosan/PAA copolymer contains the bands typical of both
241 PAA and chitosan. However, there are noticeable differences in the 1160-1020 cm⁻¹ region of the
242 spectrum that are related to the changes in the glucoside ring of chitosan [47]. To gain a more
243 detailed understanding of the changes occurring in chitosan molecules during copolymer
244 formation, the difference spectrum was obtained by subtracting the PAA spectrum from the



245 chitosan/PAA copolymer spectrum (Figure 2).

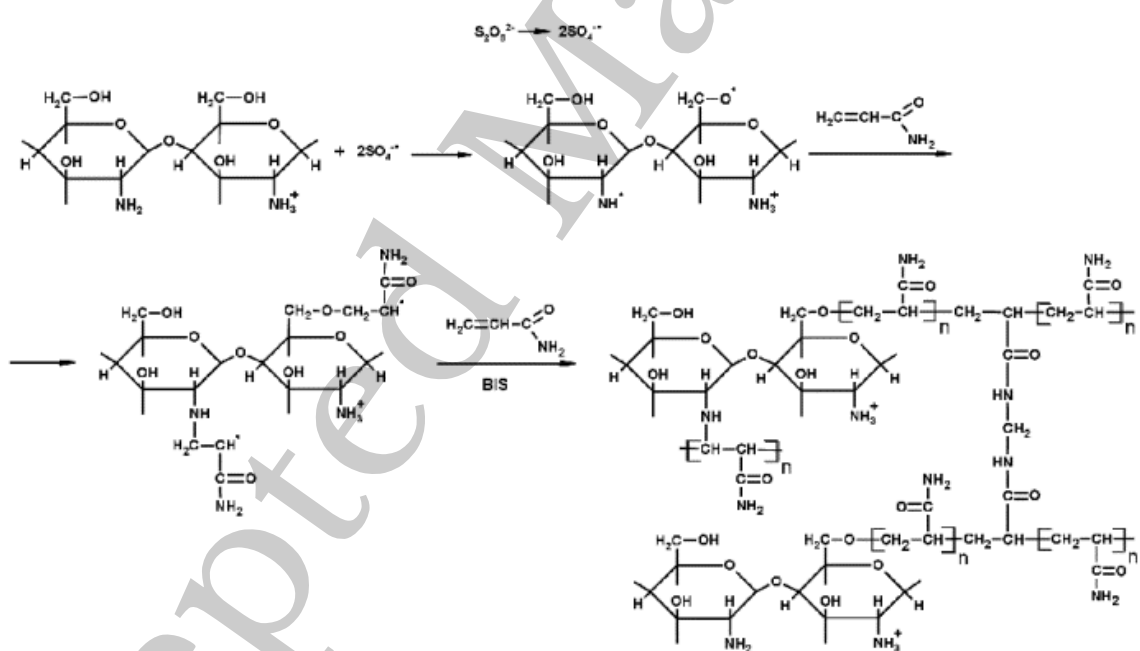
246 **Fig. 2.** FTIR spectrum of chitosan (1) and the difference spectrum obtained by subtracting the
247 PAA spectrum from the chitosan/PAA copolymer spectrum (2).

248

Disclaimer: This is not the final version of the article. Changes may occur when the manuscript is published in its final format.

When comparing the chitosan spectrum (1) and the difference spectrum (2), the shifts of the following bands: from 1150 cm^{-1} to 1160 cm^{-1} , from 1067 cm^{-1} to 1052 cm^{-1} , and from 1020 cm^{-1} to 1030 cm^{-1} are seen. The variation of the shape of the spectrum in the $1240\text{-}1200\text{ cm}^{-1}$ range (Figure 2) may be explained by the appearance of the secondary amino groups (NH) in the copolymer, which agrees with the scheme of formation of copolymer with the participation of the amino groups of chitosan molecule [37].

255 The introduction of the crosslinking agent (MBAA) during copolymerization leads to the
256 formation of a crosslinked polymer structure and hydrogel formation [30]. The scheme of the
257 synthesis of the chitosan-acrylamide copolymer and crosslinking of PAA chains with N, N-
258 methylene-bis-acrylamide is presented in Figure 3.

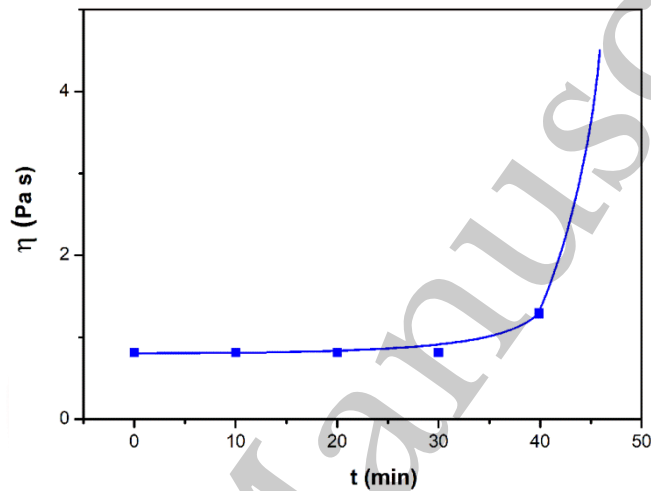


259
260
261 **Fig. 3.** Scheme of formation of the crosslinked chitosan/acrylamide copolymer.

263 Gels based on cross-linked polymers are incapable of flowing because their
264 macromolecules cannot move relative to each other. At the gelation point, the system loses
265 fluidity, and a sharp increase in the viscosity of the solution is observed. In this work, the

Disclaimer: This is not the final version of the article. Changes may occur when the manuscript is published in its final format.

266 gelation time or gel point was determined by the rheological method. The dependence of shear
267 viscosity η on time t was plotted (Figure 4). It can be seen that a sharp increase in the viscosity
268 of the solution, which indicates the onset of gelation, occurs 35 min after the beginning of the
269 experiment.



270

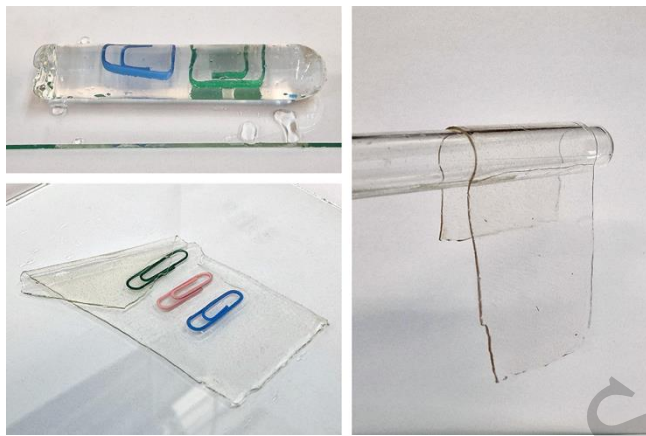
271 **Fig. 4.** Variation of viscosity of the chitosan/PAA solution with time.

272

273 3.2. The samples preparation

274 The obtained hydrogels, both cylinders and films, were colorless, transparent, and homogeneous
275 (Figure 5). The percentage of light transmission was 90-92%. The transparency of the samples
276 did not depend on the film thickness, and the swelling medium did not change during the
277 swelling process. The gap size in the frame during the film production process varied from 0.3 to
278 2 mm. After removal from the frame, the resulting films had the appropriate thickness, but
279 during the process of swelling in water, the thickness of the films increased twice.

280



281 **Fig. 5.** The photographs of different shaped gels.

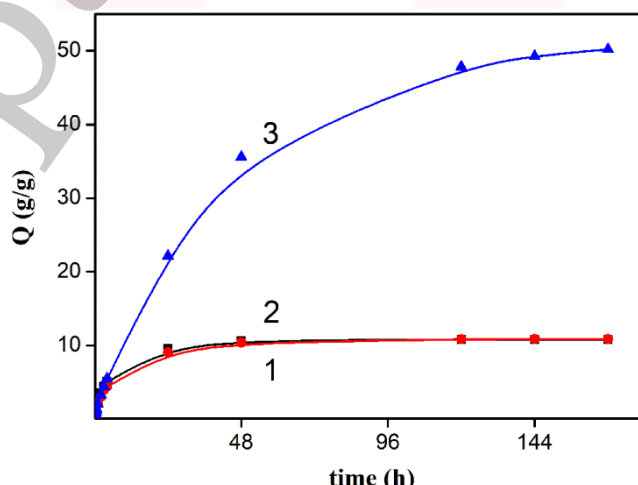
282

283 3.3. Investigation of swelling/drying process

284 A characteristic property of cross-linked polymer hydrogel structures is their ability to absorb
285 large amounts of a liquid. Such polymers swell strongly in aqueous solutions, absorbing and
286 retaining an amount of liquid well over the dry mass of the polymer. The swelling processes of
287 the obtained chitosan/PAA hydrogels were investigated in a wide pH range of the medium. The
288 hydrogel samples showed the same degree of equilibrium swelling regardless of their shape
289 [48,49].

290 Figure 6 presents the plots of swelling Kinetics of the chitosan/PAA hydrogel samples in
291 aqueous solutions with pH = 2.1 (0.1 M HCl), pH = 6.8 (H₂O dist.), and pH = 12.8 (1 M NaOH).

292



Disclaimer: This is not the final version of the article. Changes may occur when the manuscript is published in its final format.

293 **Fig. 6.** Swelling Kinetics of the chitosan/PAA hydrogel samples in aqueous solutions with pH =
294 2.1 (1), pH = 6.8 (2), and pH = 12.8 (3)

295

296 The swelling degree of the samples increases sharply at all pH values during the initial
297 stage, indicating a high rate of solvent diffusion into the gel. It then reaches a plateau, signifying
298 the attainment of equilibrium swelling (Q_e). The time required to reach the Q_e was similar in
299 acidic and neutral media. In an alkaline solution, Q_e was reached for a longer time and achieved
300 a higher value of the equilibrium swelling degree. This is because during swelling in alkali, on
301 the one hand, hydrolysis of PAA and partial conversion of amide groups into carboxylate groups
302 (COO^-) occurs, and on the other hand, chitosan in the hydrogel exists in the salt form and
303 contains acetate groups (CH_3COO^-) in the chain. Upon dissociation of such hydrogel in aqueous
304 solution, the groups carrying charge and counterions are formed. The charged ions in
305 macromolecules are bound to the polymer chains, while counterions remain in the solution in a
306 free state. Due to repulsion between similarly charged units of the spatial network, separation of
307 polymer chains and stretching of the network take place, which eventually results in a high
308 swelling degree [50].

309 The equilibrium swelling degree of gels in water is much lower than that in alkali. The
310 obtained hydrogel is a weak polyelectrolyte and poorly dissociates into ions in aqueous solution.
311 The polymer network is subjected to a lower deformation degree than that during swelling in
312 alkali, which hinders the diffusion of the solution into the hydrogel.

313 In an acidic medium, ionization of carboxyl and acetate groups is suppressed due to the
314 presence of excess hydrogen ions; the macromolecule acquires a positive charge, which leads to
315 shielding of charge and weak swelling in an acidic medium.

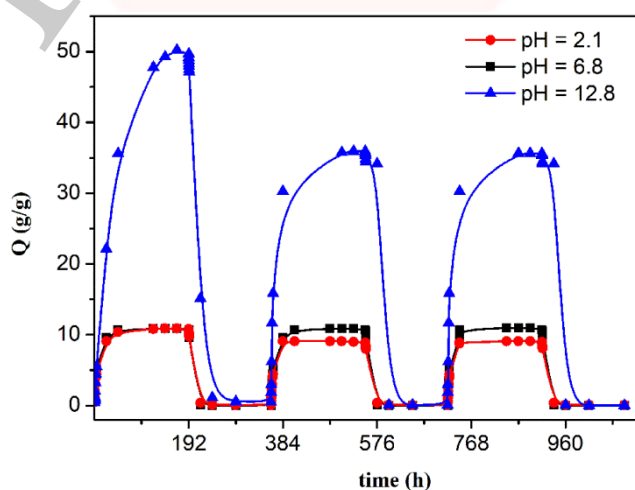
316 After swelling, the hydrogels were dried, and the change in mass of the dried sample after
317 swelling compared to the initial sample was monitored. It was found that the swelling process is
318 completely reversible in acidic and neutral media. The mass of the sample after the swelling-

Disclaimer: This is not the final version of the article. Changes may occur when the manuscript is published in its final format.

319 drying cycle was equal to the initial mass. After drying the samples swollen in the alkaline
320 medium, an increase in the sample mass was observed compared to the initial one. An increase
321 in the mass of the dried sample after 3 cycles of swelling-drying was 53%, while the main
322 increase in the mass of the samples occurring after the first cycle was 45%. The observed effect
323 is a result of the interaction of hydrogel components with alkali and salt formation.

324 The dried samples were subjected to a repeated swelling-drying cycle. It was shown that
325 in the neutral medium, the repetitive swelling process did not differ from the first cycle. In the
326 acidic medium, a slight reduction in the equilibrium swelling degree was observed during the
327 second cycle. The observed effect may be explained by the fact that during the first swelling of
328 the hydrogel in acid, partial acidic hydrolysis occurred, and acidic groups were formed in the
329 polymer chain. Upon repeated immersion of the sample into an acid solution, the positively
330 charged ions of the surrounding solution were shielded by the hydrogel surface, which prevented
331 their diffusion.

332 In an alkaline environment, a decrease in the degree of equilibrium swelling was
333 observed in the second cycle and is maintained in subsequent cycles. This is because not the
334 initial hydrogel, but the salt of the corresponding acid formed during the first cycle, undergoes
335 repeated swelling. As a result, the sodium ions located in the environment of the hydrogel
336 repulse similarly charged ions of the solution [51]. The cyclic character of the swelling-drying
337 processes is illustrated in Figure 7.



Disclaimer: This is not the final version of the article. Changes may occur when the manuscript is published in its final format.

339 **Fig. 7.** Cycles of the swelling-drying process of the chitosan/PAA hydrogel

340

341 The values of Q_e depending on the pH of the swelling medium are presented in Table 1.

342

343 **Table 1.** The equilibrium degree of swelling in media of different pH

pH	Q_1 , g/g	Q_2 , g/g	Q_3 , g/g
2.1	10.9	9.1	9.0
6.8	10.8	11.0	11.0
12.8	50.2	36.0	36.0

344

345 3.4. Mechanical properties

346 Mechanical properties are an important characteristic of hydrogel materials for their further use.

347 The stress-strain curves under stretching and compression of the samples swollen to the

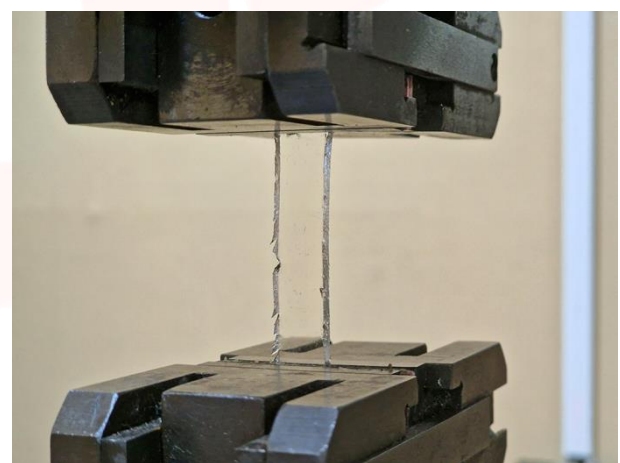
348 equilibrium state in water (pH 6.8) are presented in Figure 8. Both curves are typical for the

349 mechanical behavior of gels. The gels do not exhibit plastic deformation under either

350 compression or tension until failure.

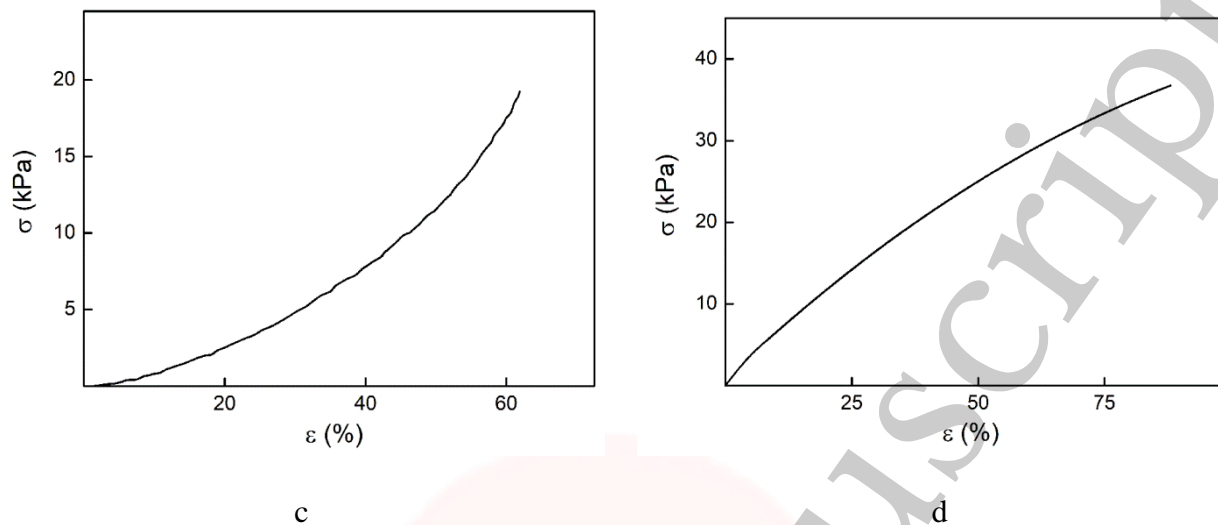


a



b

Disclaimer: This is not the final version of the article. Changes may occur when the manuscript is published in its final format.



351 **Fig. 8.** The picture of gels and stress-strain curves for (a and c) compression and (b and d)
352 stretching mode.

353

354 In order to evaluate the effect of the swelling medium on the mechanical characteristics
355 of the gels, the samples swollen to the equilibrium state in media with pH 2.1 and 12.8 were
356 tested. The obtained stress-strain curves were used to calculate the mechanical characteristics of
357 the gels under compression and stretching. The values of mechanical characteristics are shown in
358 Table 2.

359

360 **Table 2.** Mechanical characteristics of hydrogels depending on pH*

pH	Degree of swelling, Q, g/g	Breaking strength, σ , kPa	Elastic modulus, G, kPa	Deformation at break, ε , %
2.1	10.9	23.8 / 41	3.35 / 61	68 / 91
6.8	10.8	19.1 / 37	3.31 / 57	62 / 88
12.8	50.2	5.3 / 11	1.82 / 32	46 / 63

361 * The numerator shows the characteristics for compression mode, and the denominator –
362 stretching mode.

Disclaimer: This is not the final version of the article. Changes may occur when the manuscript is published in its final format.

363

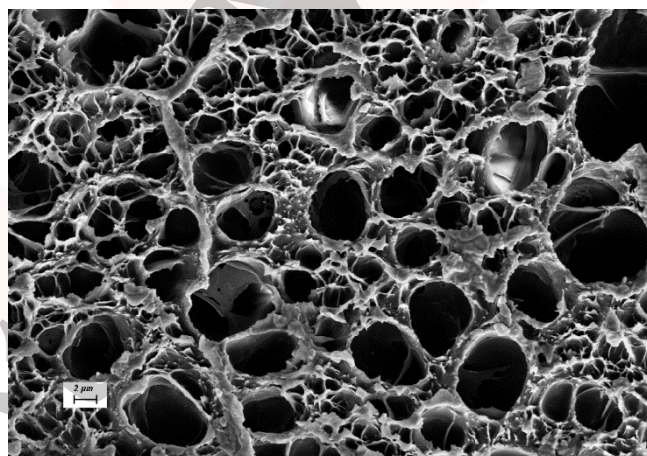
364 As follows from Table 2, the hydrogels swollen in the alkaline medium have lower
365 mechanical characteristics compared to those swollen in acidic and neutral media. In the alkaline
366 solution, the gels demonstrate the highest swelling degree, i.e., the network is substantially
367 deformed, which leads to a drop in mechanical properties.

368

369 3.5 Biological activity

370 Since the prepared hydrogels are intended for use in tissue engineering, special attention should
371 be paid to their biocompatibility and bioactivity [52]. In addition, such materials should possess
372 a porous structure to ensure cell adhesion and proliferation.

373 The SEM studies revealed that these samples have a developed porous surface with
374 micron- and submicron-sized pores (Figure 9).



375

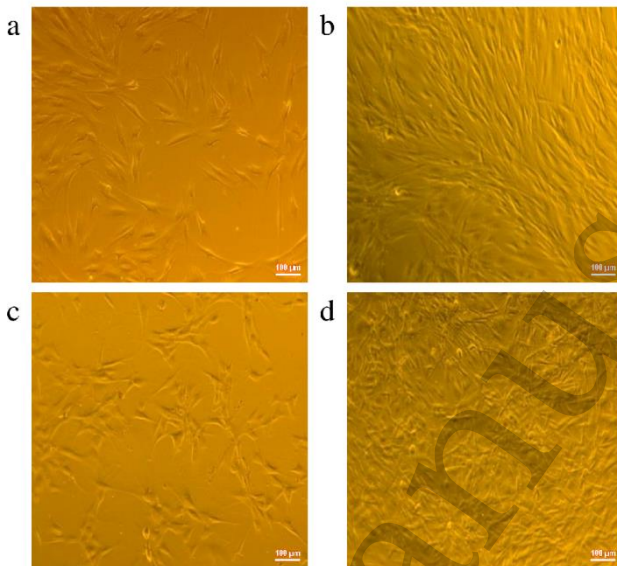
376 **Fig. 9.** SEM micrographs of the chitosan/PAA hydrogel surface

377

378 The biological activity of the obtained hydrogels was estimated by the MTT test. The
379 material was sterilized by autoclaving for 35 min at 120 °C. The samples were soaked in the
380 DMEM nutrient medium with the addition of 1 % L-glutamine, 1 % antibiotics, 1 % fungizone,
381 and 10 % fetal calf serum according to the standard method. Human dermal fibroblasts were

Disclaimer: This is not the final version of the article. Changes may occur when the manuscript is published in its final format.

382 seeded on the surface of the material in an amount of $30 \cdot 10^3$ wells. The morphology and growth
383 pattern of the cells were recorded using light microscopy (Figure 10).



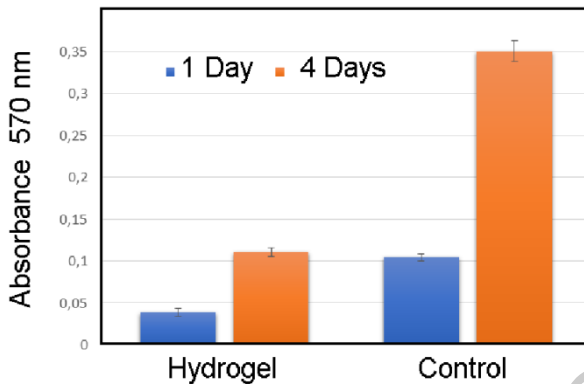
384

385 **Fig. 10.** (a and b) Images of human dermal fibroblasts grown on the surface of culture plate and
386 (c and d) chitosan/PAA hydrogel matrices after (a and c) 1 and (b and d) 4 days of cultivation.

387

388 The presented images show that the morphology and wettability of the obtained
389 hydrogels are suitable for efficient cell growth.

390 After the first and the fourth days of cultivation, 100 μ L of MTT working solution (5
391 mg/mL in DPBS) was added to the samples, and they were incubated for 2 h. 1 mL of DMSO
392 was used to dissolve formazan crystals. The resulting solution was stirred thoroughly and
393 incubated for 5 min, then optical density measurements were performed. The data of the MTT
394 test are presented in Figure 11.



395

396 **Fig. 11.** Viability and proliferation of human dermal fibroblasts on surfaces of hydrogels and
397 cultural polystyrene surface (control) as determined by MTT assay. MTT test involved human
398 dermal fibroblasts cultured on control and on the surface of the chitosan/PAA hydrogel matrices
399 for 1 and 4 days. Optical density correlates with the number of viable cells. * p < 0.05.

400

401 As can be seen in the histogram, the optical density of the solution taken from the
402 hydrogel matrices is lower than that taken from the cultural plate. Therefore, cell growth in the
403 obtained samples is less intensive. Comparing the first and the fourth days of cultivation, the
404 proliferation of human fibroblasts on the chitosan/PAA gels is clearly visible, which indicates
405 the viability of cells on the studied hydrogel matrices.

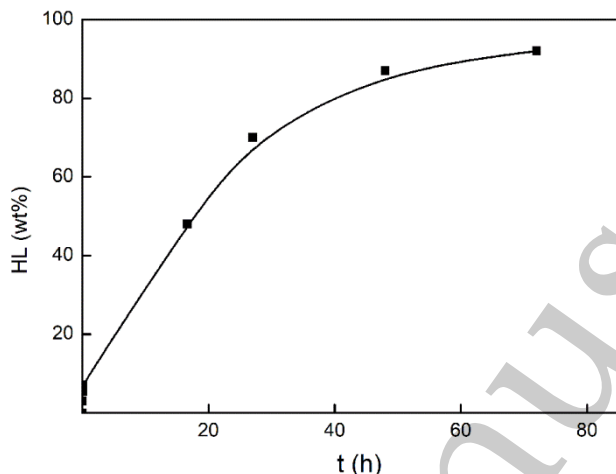
406

407 3.6 Drug release

408 In this work, the possibility of using the obtained chitosan/PAA systems for the controlled
409 release of drugs from the polymer matrix was studied using a lidocaine hydrochloride (HL)
410 solution as a model compound. The kinetics of the HL release from the chitosan/PAA hydrogel
411 in phosphate buffer at 37 °C is shown in Figure 12. The results show that the highest drug
412 release rate occurs in 30-40 min. This may be because the drug from the border regions of the
413 hydrogel is released first. Then the drug release occurs by diffusion from the hydrogel volume,
414 which results in a lower rate of the process. The release of HL from the hydrogel continues for
415 80 h and reaches 90%. The observed prolonged release of the drug can be explained by the fact

Disclaimer: This is not the final version of the article. Changes may occur when the manuscript is published in its final format.

416 that at swelling, the dry hydrogel absorbs a significant amount of HL (up to 15 g/g), filling the
417 entire volume of the gel.



418

419 **Fig. 12.** Amounts of HL released from chitosan/PAA hydrogels into the physiological solution at
420 37 °C.

421

422 **4. Conclusions**

423

424 In this work, biocompatible swelling hydrogels comprised of a natural polymer, chitosan, and a
425 synthetic one, polyacrylamide, were obtained. The possibility of obtaining hydrogel materials of
426 various shapes was demonstrated. The dependence of the swelling degree on the pH of the
427 medium was studied, and the reversibility of the swelling/drying process was analyzed for
428 chitosan/PAA systems. The conditions for achieving the minimum and maximum values of the
429 equilibrium degree of swelling are established. It was shown that the highest values of the
430 equilibrium degree of swelling were obtained for samples in an alkaline medium. Besides, the
431 pH of the media affects the mechanical characteristics of synthesized hydrogels. Thus, gels
432 swollen in an alkaline medium exhibit lower mechanical strength than those swollen in acidic
433 and neutral media due to their higher degree of swelling in alkaline solutions. However, it should
434 be noted that the hydrogels retain mechanical stability and elasticity in all the media studied. The
435 biocompatibility of the obtained hydrogels was confirmed by the MTT test. Using the HL as a

Disclaimer: This is not the final version of the article. Changes may occur when the manuscript is published in its final format.

436 model compound, it was shown that synthesized hydrogels can be considered effective matrices
437 for prolonged drug release.

438 **List of Abbreviations**

439 FTIR - Fourier transform Infrared Spectroscopy

440 PAA - Polyacrylamide

441 AA - Acrylamide

442 APS - Ammonium Peroxydisulfate

443 TEMED - N, N, N', N'-Tetramethylethylenediamine

444 MBAA - N, N'-Methylene-bis-acrylamide

445 ATR - Attenuated Total Reflectance

446 HL - Lidocaine Hydrochloride

447 SEM - Scanning Electron Microscopy

448 DMEM - Dulbecco's Modified Eagle Medium

449 DPBS - Dulbecco's Phosphate-Buffered Saline

450 DMSO – Dimethylsulfoxide

451

452 **Author Contributions.** Conceptualization, E.R., Z.Z., and N.S.; methodology, Z.Z., E.R., E.V.,
453 I.K., K.K., N.S.; Investigation, E.R., Z.Z., E.V., E.V., I.K., N.S., K.K., N.S.; Writing—Original
454 Draft Preparation, E.R., E.V., E.V., I.K.; Writing—Review & Editing, E.R., I.K. and Z.Z.;
455 Supervision, E.R., I.K. and Z.Z.

456 **Data availability statement.** The data that support the findings of this study are available from
457 the corresponding author upon reasonable request.

458

459 **Ethics Committee approval and consent to participate.** Ethical approval was not necessary
460 because the cell culture obtained from the Vertebrate Cell Culture Collection of the Institute of
461 Cytology of the Russian Academy of Sciences was used for the study.

Disclaimer: This is not the final version of the article. Changes may occur when the manuscript is published in its final format.

462

463 **Funding.** The work was carried out within the state assignment of the Institute of
464 Macromolecular Compounds - Branch of Petersburg Nuclear Physics Institute named by B.P.
465 Konstantinov of National Research Centre «Kurchatov Institute» - 124013000728-0.

466

467 **Conflicts of interest.** The authors declare no conflicts of interest.

468 **Acknowledgments:** Declared none.

469

470

471 **References**

472 [1] S. Ajmal, F. Hashmi, I. Imran, “Recent progress in development and applications of
473 biomaterials” *Materials Today: Proceedings* (2022).<https://doi.org/10.1016/j.matpr.2022.04.233>.

474 [2] SH. Aswathy, U. Narendrakumar, I. Manjubala, ‘Commercial hydrogels for biomedical
475 applications” *Helixon* 6(4):e03719. 2020. <https://doi.org/10.1016/j.heliyon.2020.e03719>

476 [3] T. Eoin, A. Maura, M. Anne, W. Gerard, “Nature-Based Biomaterials and their application in
477 Biomedicine” *Polymers* 13(19): 3321. 2021; <https://doi.org/10.3390/polym13193321>.

478 [4] M. Nagpal, SK. Singh, D. Mishra, “Superporous hybrid hydrogels based on polyacrylamide
479 and chitosan: Characterization and in vitro drug release” *Int J Pharm Investig.* 2013.
480 <https://doi.org/10.4103/2230-973X.114906>.

481 [5] T. Billiet, M. Vandenhante, J. Schelfhout, S. Van Vlierberghe, P. Dubruel, “A review of
482 trends and limitations in hydrogel-rapid prototyping for tissue engineering” *Biomaterials*.2012.
483 <https://doi.org/10.1016/j.biomaterials.2012.04.050>.

484 [6] Q. Chai, Y. Jiao, X. Yu, “Hydrogels for Biomedical Applications: Their Characteristics and
485 the Mechanisms behind Them” *Gels*, 2017. <https://doi.org/10.3390/gels3010006>

486 [7] EM. Ahmed, “Hydrogel: Preparation, characterization, and applications”: A review *J Adv.*
487 *Res.* 2015. <https://doi.org/10.1016/j.jare.2013.07.006>.

Disclaimer: This is not the final version of the article. Changes may occur when the manuscript is published in its final format.

488 [8] N. Beheshtizadeh, N. Lotfibakhshaiesh, Z. Pazhouhnia, M. Hoseinpour, M. Nafaril, “A
489 review of 3D bio-printing for bone and skin tissue engineering: A commercial approach”. *J
490 Mater Sci.* 55, pp. 3729-3749, 2020. <https://doi.org/10.1007/s10853-019-04259-0>

491 [9] F. Wenzhuo, Y. Ming, W. Liyang, L. Wenyaoyao, L. Meng, J. Yangwang et al, “Hydrogels for
492 3D bioprinting in tissue engineering and regenerative medicine: Current progress and
493 challenges” *IJB*. 2023. <https://doi.org/10.18063/ijb.759>

494 [10] A.S. Hoffman, “Hydrogels for biomedical applications” *Adv. Drug Deliv. Rev.* 43, pp. 3-12,
495 2002. [https://doi.org/10.1016/s0169-409x\(01\)00239-3](https://doi.org/10.1016/s0169-409x(01)00239-3)

496 [11] J. Liang, P. Dijkstra, A. Poot, D. Grijma, “Hybrid Hydrogels Based on Methacrylate-
497 Functionalized Gelatin (GelMA) and Synthetic Polymers”. *Biomedical Materials &
498 Devices*. vol.1, pp.191-201, 2023. <https://doi.org/10.1007/s44174-022-00023-2>

499 [12] H. Li, K. Zhao, J. Jiang, Q. Zhu, “Research progress on black phosphorus hybrids hydrogel
500 platforms for biomedical applications” *J Biol Eng.*, vol.17,8, pp. 1-18, 2023.
501 <https://doi.org/10.1186/s13036-023-00328-w>

502 [13] Q. Feng, K. Zhang, B. Yang, Y. Yu, Editorial: “Biomedical applications of natural
503 polymers” *Front. Bioeng. Biotechnol*, vol. 10, 2022. <https://doi.org/10.3389/fbioe.2022.1077823>

504 [14] E. Maria, “A review of chitosan-, alginate-, and gelatin-based biocomposites for bone tissue
505 engineering” *Biomaterials and Tissue Engineering Bull.*, vol. 5, (3-4): pp. 97-109, 2018.
506 <https://doi.org/10.33263/BTEB534.097109>

507 [15] A. Mochalova, L. Smirnova, “State of the Art in the Targeted Modification of Chitosan”
508 *Polym. Sci. Ser. B*, vol.60. pp.131-161, 2018. <https://doi.org/10.1134/S1560090418020045>

509 [16] S. Dutta, D. Patel, K. Lim, “Functional cellulose-based hydrogels as extracellular matrices
510 for tissue engineering” *J Biol Eng*, 13, 55, 2019. <https://doi.org/10.1186/s13036-019-0177-0>

511 [17] MCG. Pellá, MK. Lima-Tenório, ET. Tenório-Neto, MR. Guilherme, EC. Muniz, AF.
512 Rubira, “Chitosan-based hydrogels: From preparation to biomedical applications” *Carbohydr
513 Polym.* 2018. <https://doi.org/10.1016/j.carbpol.2018.05.033>.

Disclaimer: This is not the final version of the article. Changes may occur when the manuscript is published in its final format.

514 [18] M. Azmana, S. Mahmood, AR. Hilles, A. Rahman, MAB. Arifn, S. Ahmed, “A review on
515 chitosan and chitosan-based bionanocomposites: promising material for combatting global issues
516 and its applications” *Int. J. Biol. Macromol.* 185: pp. 832–848, 2021.
517 <https://doi.org/10.1016/j.ijbiomac.2021.07.023>

518 [19] A. Alicia, Z. Naimah, H. Ezeddine, H. Brahim, B. Fabien, O. Damien et al., “Application of
519 Chitosan in Bone and Dental Engineering” *Molecules*, 19; 24(16), 3009, 2019.
520 <https://doi.org/10.3390/molecules24163009>

521 [20] BE. Mirzaei, SAA. Ramazani, M. Shafiee, M. Danaei, “Studies on Glutaraldehyde
522 Crosslinked Chitosan Hydrogel Properties for Drug Delivery Systems” *Int. J. of Polymeric
523 Materials and Polymeric Biomaterials*, 19; 24(16):3009, 2013.
524 <https://doi.org/10.1080/00914037.2013.769165>.

525 [21] M. Arteche Pujana, L. Pérez-Álvarez, LC. Cesteros Iturbe, I. Katime, “Biodegradable
526 chitosan nanogels crosslinked with genipin” *Carbohydr. Polym.* 15;94 (2):836-42, 2013.
527 <https://doi.org/10.1016/j.carbpol.2013.01.082>

528 [22] T. Guoke, T. Zhihong, Z. Wusi, W. Xing, S. Changgui, L. Yi, H. Hailong et al., “Recent
529 Advances of Chitosan-Based Injectable Hydrogels for Bone and Dental Tissue Regeneration”
530 *Front. Bioeng. Biotechnol*, 2020. <https://doi.org/10.3389/fbioe.2020.587658>

531 [23] U. Özügür , Ş. Nayır, M. Açıba, B. Çitır, S. Durmaz, Ş. Koçoğlu et al., “2D Materials (WS₂,
532 MoS₂, MoSe₂) Enhanced Polyacrylamide Gels for Multifunctional Applications” *Gels*.
533 8(8):465.2022. <https://doi.org/10.3390/gels8080465>.

534 [24] S. Azizian, A. Hadjizadeh, H. Niknejad, “Chitosan-gelatin porous scaffold incorporated
535 with Chitosan nanoparticles for growth factor delivery in tissue engineering”. *Carbohydrate
536 Polymers*. 15:202:pp. 315-322, 2018. <https://doi.org/10.1016/j.carbpol.2018.07.023>

537 [25] Y. Boguang, X. Jingwen; Zh. Kunyu, “Multicomponent Hydrogels for Tissue Engineering
538 Applications” In book: Multicomponent Hydrogels Series: Biomaterials Science Series, pp.346-
539 380, 2023. <https://doi.org/10.1039/BK9781837670055-00346>

Disclaimer: This is not the final version of the article. Changes may occur when the manuscript is published in its final format.

540 [26] A. Tangri, "Polyacrylamide based hydrogels: synthesis, characterization and applications.
541 International journal of pharmaceutical, chemical and biological sciences" *Materials Science,*
542 *Medicine*, 4(4):pp. 951-959, 2014.

543 [27] Y. Kaiji, C. Jinghuan, F. Qingjin, D. Xuji, Y. Chunli, "Preparation of novel amphoteric
544 polyacrylamide and its synergistic retention with cationic polymers" *E-Polymers*, 20(1): pp. 162-
545 170, 2020. <https://doi.org/10.1515/epoly-2020-0026>

546 [28] B. Robina, H. Zahoor, A. Ejaz, S. Ahsan, W. Weitai, I. Ahmad, "Fundamentals and
547 applications of acrylamide based microgels and their hybrids" A review. *RSC Adv.* 7;9(24):
548 pp.13838-13854, 2019. <https://doi.org/10.1039/C9RA00699K>

549 [29] C. Mihăilescu A. Dumitrescu, B. Simionescu, V. Bulacovschi, "Synthesis of
550 polyacrylamide-based hydrogels by simultaneous polymerization/crosslinking" *Rev. Roum.*
551 *Chim.* 52(11): pp. 1071-1076, 2007.

552 [30] V. Lopatin, A. Askadskii, A. Peregudov, V. Berestnev, A. Shekhter, "Structure and
553 properties of polyacrylamide gels for medical applications" *Polymer science Series A* vol.46,
554 (12): pp. 1282-1292, 2004.

555 [31] J. Zhang, B. Jing, G. Tan, S. Fang, H. Wang, "Effect of Structure of Graft on the Properties
556 of Graft Copolymers of Acrylamide and Surfactant Macromonomers Dilute Aqueous Solutions"
557 *J. Macromol. Sci., Part B, Phys.* 54(3): pp. 253-261, 2015.
558 <https://doi.org/10.1080/00222348.2014.1000798>

559 [32] G. Ma, X. Li, X. Wang, G. Liu, L. Jiang. K. Yang, "Preparation, rheological and drag
560 reduction properties of hydrophobically associating polyacrylamide polymer" *J. Dispersion Sci.*
561 *Technol.* 40(2), pp. 1-8, 2018. <https://doi.org/10.1080/01932691.2018.1461637>

562 [33] P. Kesharwani, A. Bisht, A. Alexander, V. Dave, S. Sharma, "Biomedical applications
563 of hydrogels in drug delivery system": An update. *Journal of Drug Delivery Science and*
564 *Technology*. 66(2):102914. 2021. <https://doi.org/10.1016/j.jddst.2021.102914>

Disclaimer: This is not the final version of the article. Changes may occur when the manuscript is published in its final format.

565 [34] H. Shoukat, K. Buksh, S. Norean, F. Pervaiz, I. Maqbool, "Hydrogels as potential drug-
566 delivery systems: network design and applications' *Ther Deliv* 12(5): pp. 375-396, 2021.
567 <https://doi.org/10.4155/tde-2020-0114>

568 [35] A. Mochalova, L. Smirnova, S. Zaitsev, Yu. Semchikov, I. Zaitseva, G. Pavlov,
569 "Hydrodynamic and molecular characteristics of graft copolymers of chitosan with acrylamide"
570 *Polym. Sci. Ser. B*. vol. 49, pp. 232-235, 2007. <https://doi.org/10.1134/S1560090407090059>

571 [36] A. Mochalova, N. Zaborshchikova, A. Knyazev, L. Smirnova, Yu. Semchikov, "Graft
572 polymerization of acrylamide on chitosan: Copolymer structure and properties". *Polym. Sci.*
573 *Ser.A*. vol.48, pp. 918–923, 2006. <https://doi.org/10.1134/S0965545X06090069>

574 [37] L. Bellamy, The Infra-red spectra of complex molecules Methuen: London, Wiley, New
575 York. 1963.

576 [36] Sánchez-Cid, P.; Jiménez-Rosado, M.; Romero, A.; Pérez-Puyana, V. Novel Trends in
577 Hydrogel Development for Biomedical Applications: Review. *Polymers*, 2022, 14(15), 3023.
578 <https://doi.org/10.3390/polym14153023>

579 [37] Carpa, R.; Farkas, A.; Dobrota, C.; Butiuc-Keul, A. Double-Network Chitosan-Based
580 Hydrogels with Improved Mechanical, Conductive, Antimicrobial, and Antibiofouling
581 Properties. Review, *Gels*, 2023, 9(278), 1-21. <https://doi.org/10.3390/gels9040278>

582 [38] Xu, X.; He, C.; Luo, F.; Wang, H.; Peng, Z. Transparent, Conductive Hydrogels with High
583 Mechanical Strength and Toughness. *Polymers*, 2021, 13(12), 2004.
584 <https://doi.org/10.3390/polym13122004>

585 [39] Wu, K.Y.; Akbar, D.; Giunta, M.; Kalevar, A.; Tran, S.D. Hydrogels in Ophthalmology:
586 Novel Strategies for Overcoming Therapeutic Challenges. *Materials*, 2024, 17(1), 86.
587 <https://doi.org/10.3390/mal17010086>

588 [40] Mitura, S.; Sionkowska, A.; Jaiswal, A. Special issue: Hydrogels in regenerative medicine
589 Review Article Biopolymers for hydrogels in cosmetics: Review. *Journal of Materials Science:*
590 *Materials in Medicine*, 2020, 31(50). <https://doi.org/10.1007/s10856-020-06390-w>

Disclaimer: This is not the final version of the article. Changes may occur when the manuscript is published in its final format.

591 [41] Chao, M.; Yehang, D.; Ruiling, L.; Lufeng, Z.; Ziqi, Zh.; Silin, G; et al. . Carboxymethyl
592 chitosan/polyacrylamide double network hydrogels based on hydrogen bond cross-linking as
593 potential wound dressings for skin repair. *Int J Biol Macromol*, 2024, 280 (Pt 2).
594 <https://doi.org/10.1016/j.ijbiomac.2024.135735>.

595 [42] Bingyang, L.; Xiao, H.; Dan, Z.; Xiao, L.; Li, L.; Jingyue, W.; et al. Catechol-
596 chitosan/polyacrylamide hydrogel wound dressing for regulating local inflammation. *Mater*
597 *Today Bio*, 2022. 16(2). <https://doi.org/10.1016/j.mtbiol.2022.100392>

598 [43] Chamkouri, H.; Chamkouri, M. A Review of Hydrogels, Their Properties and Applications
599 in Medicine. *Am. J. Biomed. Sci. & Res.*, 2021, 11(6), 485-493.
600 <https://doi.org/10.34297/AJBSR.2021.11.001682>

601 [44] Ward, I.M. *Mechanical properties of solid polymers* / I.I.Ward, J.Sweeney. - 3th ed. -
602 Hoboken: Wiley, 2012.

603 [45] Brugnerotto, J.; Lizardi, J.; Goycoolea, F.; Arguelless -Monal, W.; Desbrieres J., Rinaudo
604 M., An infrared investigation in relation with chitin and chitosan characterization, *Polymer*,
605 2001, 42(8), 3569-3580. [https://doi.org/10.1016/S0032-3861\(00\)00713-8](https://doi.org/10.1016/S0032-3861(00)00713-8)

606 [46] Gaabour, L. Spectroscopic and thermal analysis of polyacrylamide/chitosan (PAM/CS)
607 blend loaded by gold nanoparticles. *Results in Physics*, 2017, 7, 2153–2158.
608 <https://doi.org/10.1016/j.rinp.2017.06.027>.

609 [47] Van de Velde, K.; Kiekens, P. Structure analysis and degree of substitution of chitin,
610 chitosan and dibutyrylchitin by FT-IR spectroscopy and solid state ¹³C NMR, *Carbohydr.*
611 *Polym*, 2004, 58(4), 409-416. <https://doi.org/10.1016/j.carbpol.2004.08.004>

612 [48] Xie, J.; Liu, X.; Liang J.; , Luo, Yi. Swelling Properties of Superabsorbent
613 Poly(acrylicacid-co-acrylamide) with Different Crosslinkers, *Journal of Applied Polymer*
614 *Science*, 2009, 112 (2), 602–608. DOI:[10.1002/app.29463](https://doi.org/10.1002/app.29463)

Disclaimer: This is not the final version of the article. Changes may occur when the manuscript is published in its final format.

615 [49] Huang Sh.; Shen, Ji.; Li N.;, Yeformat, M. Dual pH- and temperature-responsive hydrogels
616 with extraordinary swelling/deswelling behavior and enhanced mechanical performances,
617 *Journal of Applied Polymer Science*, 2014, 132 (9). <https://doi.org/10.1002/app.41530>

618 [50] Zhoua, Yu.; Jin, Li. Hydrolysis-induced large swelling of polyacrylamide hydrogels, *Soft*
619 *Matter*, 2020, 16, 5740-5749. <https://doi.org/10.1039/D0SM00663G>

620 [51] Rohindra, D.; Nand, A.; Khurma, J. Swelling properties of chitosan hydrogels. *The South*
621 *Pacific Journal of Natural and Applied Sciences*, (2004), 22(1), 32-35.
622 <https://doi.org/10.1071/sp04005>

623 [52] Hou, W.; Yu, X.; Li, Ya; Wei, Yi.; Ren, Ju. Ultrafast Self-Healing, Highly Stretchable,
624 Adhesive, and Transparent Hydrogel by Polymer Cluster Enhanced Double Networks for Both
625 Strain Sensors and Environmental Remediation Application. *ACS Applied Materials &*
626 *Interfaces* (Surfaces, Interfaces, and Applications), 2022, 14(51), 57387-57398.
627 <https://doi.org/10.1021/acsami.2c17773>